Optimization of aeration conditions in the hybrid process of coagulation-ultrafiltration with air sparging

Meibo He, Chen Chen, Can Guo, Shuai Wang, Haiqing Chang and Baicang Liu

ABSTRACT

To optimize the aeration conditions in the hybrid process of coagulation-ultrafiltration with air sparging, a series of air flow rates under continuous and intermittent sparging were investigated. The water quality characteristics that surrounded membranes, bubble characteristics, fouling resistances, and energy consumption under different aeration conditions were analyzed. The results showed that increasing air flow rates generated more bubbles with a wider size distribution (i.e., more favorable hydrodynamic conditions). The turbidity and ultraviolet absorbance at 254 nm (UV_{254}) of the water that surrounded membranes were reduced as the air sparging kept flocs away from membranes. Thus, the membrane fouling was effectively mitigated by increasing air flow rates despite aeration modes. For a given air flow rate, less fouling was obtained under continuous sparging than the intermittent mode. With respect to intermittent sparging, the mode of 40-min aeration per hour more effectively alleviated membrane fouling than the mode of 30-min aeration per hour. Weighing the energy consumption and membrane fouling, optimum air flow rates under continuous mode were between 15 and 30 mL/min, and the optimal aeration condition for intermittent mode was set at the air flow rate of 30 mL/min under the mode of 40-min aeration per hour.

Key words | air sparging, hybrid process, membrane fouling, optimization, ultrafiltration

Meibo He
Can Guo
Shuai Wang
Haiqing Chang
Baicang Liu (corresponding author)
College of Architecture and Environment,
Sichuan University,
Chengdu 610207,
China
and
Institute of New Energy and Low-Carbon Technology,
Sichuan University,
Chengdu 610207,
China
E-mail: *bcliu@scu.edu.cn*

Chen Chen
Litree Purifying Technology Co., Ltd,
Haikou 571126,
China

INTRODUCTION

Ultrafiltration (UF) has gained increasing popularity in the fields of water and wastewater treatment, but membrane fouling remains inevitable. The natural organic matter (NOM) and particles in water play an important role in membrane fouling (Yamamura *et al.* 2007; Meng *et al.* 2015). Jermann *et al.* (2008) suggested that the fouling caused by the association between particles and NOM was even greater than the sum of NOM and particles fouling as the NOM serving as bridges helped the absorption of particles on the membrane. In order to alleviate the membrane fouling caused by NOM and particles, pretreatments and hydrodynamic disturbance methods have been investigated in detail.

Due to the effectivity to remove NOM and particles, the coagulation pretreatment has been applied to alleviate membrane fouling (Howe & Clark 2006; Chen *et al.* 2007). Different from the conventional drinking water treatment process, the coagulation prior to the UF process can be operated without flocculation or sedimentation, which means the coagulated water with flocs will directly enter the membrane modules. As a result, the flocs that cannot pass through the membrane pores accumulate on the membrane surface forming a porous cake layer with a relatively low hydraulic resistance (Guigui *et al.* 2002; Choi & Dempsey 2004). Additionally, the cake layer composed of flocs can absorb small flocs and uncoagulated NOM (neutral or

doi: 10.2166/aqua.2017.077

hydrophilic fraction of NOM), further reducing the membrane fouling (Guigui *et al.* 2002; Chen *et al.* 2007).

In term of hydrodynamic disturbance methods, air sparging is commonly used to mitigate membrane surface fouling by limiting the deposition of foulants on membrane surfaces (Cui *et al.* 2003). The extent of fouling mitigation is dependent on the magnitude, amount, and fluctuation of shear stress induced by air sparging (Chan *et al.* 2007, 2011). Air sparging conditions largely determine shear stress profiles and consequently have an important influence on the fouling control (Chan *et al.* 2007). On one hand, membrane fouling can be reduced with incremental air flow rates, but further increasing the air flow rate above an optimal value has little impact on the fouling reduction (Xia *et al.* 2013). On the other hand, membrane fouling can also be effectively controlled by altering the aeration mode. For instance, Abdullah *et al.* (2015) suggested that intermittent sparging could more effectively alleviate membrane fouling as it induced greater shear stress than continuous sparging did at a given air flow rate.

Although numerous studies have demonstrated that coagulation and air sparging can effectively control membrane fouling, the adverse effects of both measures on membrane fouling control have also been reported in previous literature. For example, Howe *et al.* (2006) suggested that flocs larger than 1 μm functioned as membrane foulants. On the other hand, Drews *et al.* (2010) reported that air sparging might worsen membrane fouling due to the pore blockage caused by particle classification or segregation resulting from aeration. Furthermore, most studies on the effects of coagulation or air sparging were conducted individually. Only recently have researchers recognized the integration of coagulation, air sparging, and membrane filtration as a potential way to address the problems mentioned above (Liu *et al.* 2014; Rojas-Serrano *et al.* 2015), despite Müller & Uhl (2009) doubting the ability of air sparging to eliminate membrane fouling in the coagulation-UF process.

The effect of the association between coagulation and air sparging on membrane fouling is still poorly understood. Therefore, this study was conducted to investigate the effect of aeration conditions on membrane fouling and to optimize them in the coagulation-UF with air sparging hybrid process. Specifically, this work was carried out with two objectives: (1) to investigate the effect of air flow rate and aeration mode on membrane fouling and (2) to optimize the aeration conditions in the hybrid process of coagulation-UF with air sparging.

MATERIALS AND METHODS

Materials

Surface water obtained from Mingyuan Lake in Sichuan University was used as raw water. The raw water had steady pH (8.44–8.91), slightly fluctuant turbidities (5.08–9.62 NTU), and ultraviolet absorbance at 254 nm (UV_{254}) (0.095–0.141 cm^{-1}) during all experiments.

The aluminum sulfate hydrate ($Al_2(SO_4)_3 \cdot 18H_2O$, Sigma Aldrich, reagent grade) was dissolved in ultrapure water to prepare a stock solution for coagulation with a concentration of 5 g/L as $Al_2(SO_4)_3 \cdot 18H_2O$. Ultrapure water with a resistivity of 18.2 MΩ cm was provided from an ULUPURE ultrapure water purification system (Chengdu, China). Jar tests were applied to determine the optimal coagulant dosage based on the removal of turbidity and UV_{254} for the hybrid process of coagulation-UF with air sparging.

Commercially available outside-in hollow fiber UF membranes were used in this work. Polyvinylidene fluoride membranes with an average pore size of 0.02 μm were provided by Litree Purifying Technology Co., Ltd (Haikou, China). The contact angle of the virgin membrane was 26°. The inner and outer diameters of the fibers were 1.0 and 1.8 mm, respectively. A hand-made membrane module consisting of 16 hollow fibers with an effective length of 200 mm and a total surface area of 0.018 m^2 was used in each experiment. New membranes were employed for each test. The membranes were soaked in ultrapure water for at least 24 h and rinsed carefully to remove preservatives before use.

Experimental setup

The schematic diagram of the experimental setup for the hybrid process of coagulation-UF with air sparging is shown in Figure 1. The experimental setup comprised a

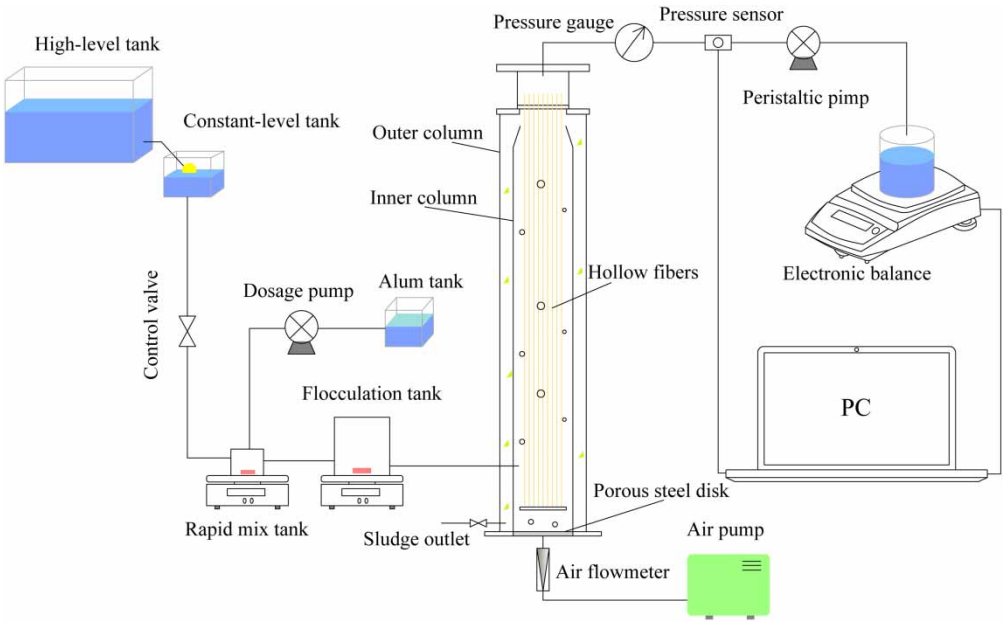

Figure 1 | Schematic diagram of the experimental setup.

high-level tank, a constant-level tank, a coagulation system, an air sparging system, a UF module, and a data recording system. The coagulation system contained a rapid mixing tank and a flocculation tank that were placed on two magnetic stirrers. The air flow was produced by an aeration pump (LP-60, Guangdong Risheng Group Co., Ltd, China) and transported into the membrane module through a gas flowmeter with a measuring range of 100 mL/min (Cole-Parmer Instrument Company, LLC, USA). Air bubbles were generated when the air flow passed through a porous steel disk (Nanjing Institute of Metallic Membrane, China) with pore sizes of 0.1–5.0 μm located at the bottom of the UF module. The UF module consisted of two cylinder columns and 16 hollow fibers. The gap between the two columns was 2 mm wide and used for the settling of flocs. Permeate water from hollow fibers was sucked by a peristaltic pump (BT100-2 J, Longer Precision Pump Co., Ltd, China). The transmembrane pressure (TMP) was simultaneously measured by a pressure sensor (UNIK 5000, General Electric Company, USA) and a pressure gauge to guarantee the accuracy of pressure data. Pressure data were collected by a Data Acquisition card and automatically recorded by a computer every 100 s. The permeate mass was acquired and logged using an electronic balance (CAV 8101, Ohaus Co., Ltd, USA) and Collect 6.1 software every minute to make sure the membrane filtration maintained a constant-flux mode.

Experimental protocol

During the coagulation, raw water was mixed with alum at the rotate speed of 300 rev/min for 1 min in the rapid mixing tank and then stirred at the rotate speed of 60 rev/min for 20 min in the flocculation tank (Liu *et al.* 2014). The optimal coagulant dosage for this hybrid process was determined at 70 mg/L as $Al_2(SO_4)_3 \cdot 18H_2O$. After coagulation, coagulated water without settling was transported into the inner column as UF feed. Membrane filtration was performed under a constant flux of 18 $L/m^2 \cdot h$ as recommended by the membrane manufacturer. A new membrane was first filtered by ultrapure water for 2 h at a constant TMP, and the membrane intrinsic resistance (R_m) was obtained in this step. Then, the feed water was filtered for 8 h. Consequently, the total resistance (R_t) (consisting of R_m, reversible resistance (R_{rev}) and irreversible resistance (R_{irr})) was determined. After the 8 h filtration, the fouled UF membranes were backwashed with ultrapure water for 5 min. Finally, the UF membranes filtered ultrapure water for another 2 h or until the flux remained constant, and the resistance including R_m and R_{irr} was determined.

During filtration, continuous or intermittent air sparging was carried out. Continuous sparging was conducted at air flow rates of 15, 30, and 60 mL/min. For intermittent sparging, two modes of 40-min aeration per hour and 30-min aeration per hour were performed at air flow rates of 30 and 60 mL/min. All tests were carried out at room temperature (25°C). In order to ensure the reliability of the experimental results, all experiments were repeated three times, and the mean values were reported.

Analytical methods

Bubble characterization

The images of bubbles were captured by a single-lens reflex camera (D7000, Nikon Co., Ltd, Japan) in the absence of the hollow fibers and the inner column. When capturing the images of bubbles, a black board was vertically placed behind the transparent outer column, and the light source was set at the top of the column. To make the measurements of bubbles as accurate as possible, each image was analyzed three times by Image Pro Plus software (Version 6.0, Media Cybernetics Inc., USA). The brightness of the images was first enhanced, then followed by the application of the erode filter to tailor the edges of bubbles and remove impurities of images. Next, the contrast of images was improved to separate bubbles from the background, and the dilate filter was used to restore the lost characterizations. The command of count/size of Image pro plus was executed to determine bubble size and number by using the diameter of the outer column as scale.

Water quality analysis

The permeate water quality including turbidity and UV_{254} was monitored during the whole experiment. As well, the water quality inside the inner column was measured because membrane fouling was mainly influenced by the water directly contacting membranes. The UV_{254} of samples prefiltered through 0.45-μm polytetrafluoroethylene membranes was measured by a UV-VIS spectrophotometer (ORION AQUAMATE 8000, Thermo Fisher Scientific Inc., USA). Turbidity was determined by a turbidimeter (2100Q, Hach, USA) using supernatant liquid after at least 30 min of settlement.

Membrane fouling resistance

In this study, resistances in series model were adapted from Kimura *et al.* (2004). In this model, the R_t which consists of R_m, R_{rev}, and R_{irr} was calculated using Equation (1):

$$R_t = R_m + R_{rev} + R_{irr} = \frac{\Delta P}{\mu J} \quad (1)$$

where J is permeate flux ($18\ L/m^2 \cdot h$), ΔP is TMP, and μ is dynamic viscosity ($0.899 \times 10^{-6}\ kPa \cdot s$).

Energy consumption

The energy consumption of air sparging was calculated according to the equation adapted from Tian *et al.* (2010):

$$E = Q \times \rho \times g \times T \times H \quad (2)$$

where E is energy consumption, Q is the air flow rate, ρ is the density of water ($997.05\ kg/m^3$), g is the gravitational acceleration ($9.81\ m/s^2$), T is the air sparging time, and H is the height of the membrane module (0.25 m).

RESULTS AND DISCUSSION

Bubble analysis

The images and the size distributions of bubbles at various air flow rates are presented in Figure 2. As shown in Figure 2(a)–2(c), the bubbles were predominantly spherical, which indicated the gas-liquid two-phase flow pattern remained as bubble flow regardless of the increase in the air flow rate. Only the number and the size distributions of bubbles differed at various air flow rates. The number of bubbles increased in the order of $15 < 30 < 60$ mL/min as displayed in Figure 2(a)–2(c). A large number of bubbles not only gave rise to more intense shear stresses (Chan *et al.* 2007) but also enhanced the number of fibers that could be affected by shear stresses. When air flow rates were low, most bubbles

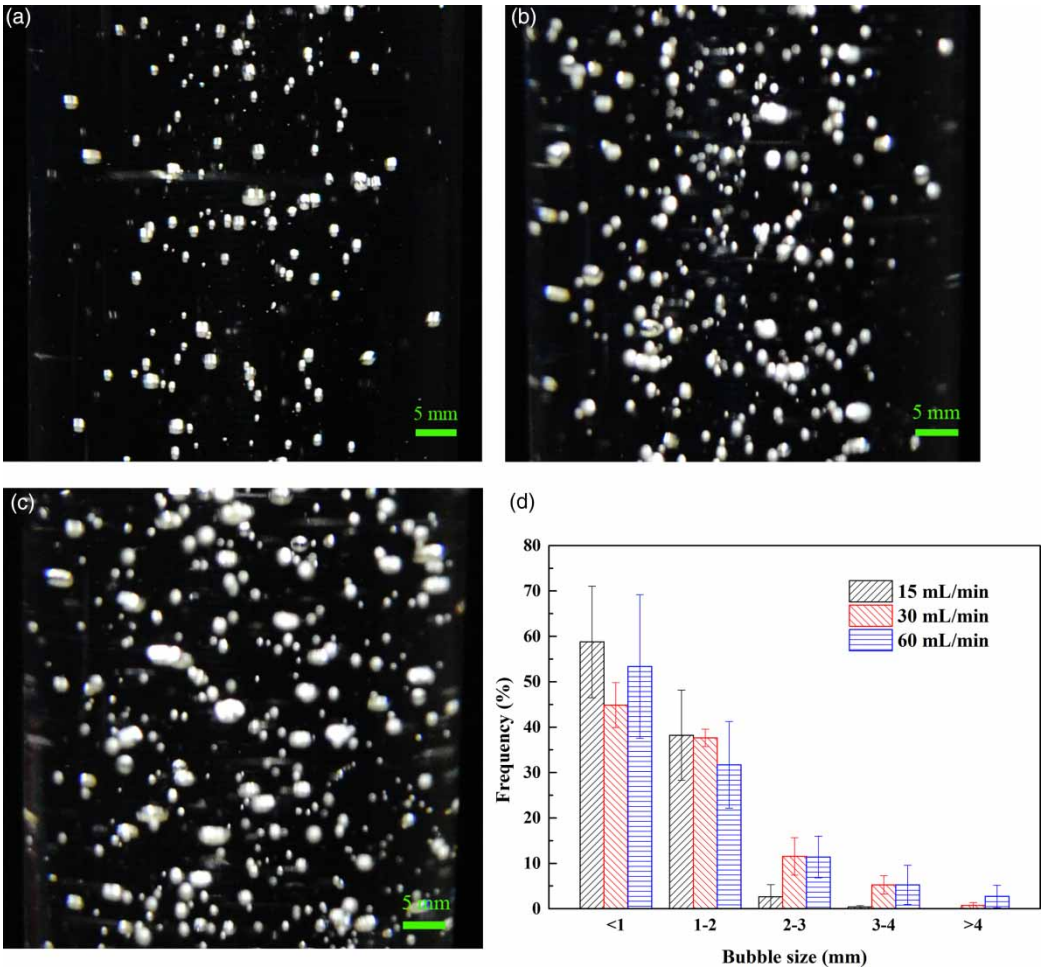

Figure 2 | Bubbles at the air flow rate of: (a) 15 mL/min; (b) 30 mL/min; (c) 60 mL/min; (d) bubble size distributions at different air flow rates (error bar indicates standard deviation).

only impacted the outer fibers and the inner fibers were sheltered from the effects of shear stresses, which resulted in the unevenly distributed fouling of hollow fibers and a consequent rapid deterioration of membrane performance (Yeo *et al.* 2006). At higher air flow rates, the shear stress induced by an increased number of bubbles affected more fibers, thus alleviating the extents of entire fouling of hollow fiber bundles on account of the less unevenly distributed fouling.

As shown in Figure 2(d), the size of bubbles was narrowly distributed at the ranges of <1 mm and 1–2 mm at the air flow rate of 15 mL/min. Bubbles with sizes of >2 mm appeared occasionally. At air flow rates of 30 and 60 mL/min, most bubbles still had sizes of <1 mm and 1–2 mm, but relatively larger bubbles with sizes of >2 mm appeared more frequently. The larger sizes and wider size ranges were able to induce greater magnitudes and stronger fluctuations of shear stresses, which were in favor of fouling control (Cui *et al.* 2003; Yeo *et al.* 2006). Although bubble sizes were similarly distributed at air flow rates of 30 and 60 mL/min, the number of bubbles at air flow rate of 60 mL/min were remarkably larger than that at air flow rate of 30 mL/min. Hence, the shear stress conditions were expected to be more advantageous to mitigate membrane fouling at air flow rate of 60 mL/min.

Water quality

During the whole experiment, the permeate water quality remained quite steady (turbidity: 0.18–0.26 NTU; UV_{254}: 0.051–0.054 cm^{-1}). These results indicate that the

membrane fouling was not severe enough to deteriorate the permeate water quality. Different from the permeate water quality, the turbidity and UV_{254} of water samples inside the inner column (i.e., the water which directly contacted but did not pass through the membranes) changed at different air flow rates. The values of turbidity and UV_{254} at air flow rates of 0, 15, 30, and 60 mL/min were 2.6, 1.4, 1.8, and 1.91 NTU, and 0.048, 0.039, 0.043, and 0.042 cm^{-1}, respectively. A part of flocs were brought out of the inner column by the gas-liquid two-phase up-flow and settled inside the gap according to the experimental observations. The turbidity and UV_{254} were slightly higher at air flow rates of 30 and 60 mL/min than those at air flow rate of 15 mL/min. The probable explanation for this is that flocs were transported into the gap without serious floc breakage as aeration was not intense at the air flow rate of 15 mL/min. However, when air flow rate increased to 30 and 60 mL/min, the enhanced hydrodynamic disturbances not only brought flocs out of the inner column but also caused part of flocs to break up inside the inner column. As the breakage of flocs might lead to the formation of small flocs and release of NOM (Liu *et al.* 2014; Rojas-Serrano *et al.* 2015), the turbidity and UV_{254} at air flow rates of 30 and 60 mL/min were higher than those at the air flow rate of 15 mL/min but still lower than those without aeration. These results indicated that the water qualities inside the inner column were improved by aeration, which in part explained the fouling mitigation as discussed below.

Effect of sparging conditions on membrane fouling

Figure 3 shows the TMP buildups and fouling resistances under different aeration conditions. As presented in Figure 3(a), under the continuous sparging, the dTMP/dT at the air flow rates of 0, 15, 30, and 60 mL/min were 0.83, 0.58, 0.29, and 0.25 kPa/h, respectively, indicating that increasing air flow rate led to the reduction of membrane fouling. These results agree well with the bubble analysis. The bubbles generated at higher air flow rates produced more favorable hydrodynamic conditions and thereby led to less severe membrane fouling. Although the turbidity and UV_{254} increased as the air flow rate varied from 15 to 30 mL/min, the fouling was still reduced, which indicated that the increased turbidity and UV_{254} at the air flow rate of 30 mL/min were not deleterious enough to offset the positive effects of shear stresses on mitigating membrane fouling. When the air flow rate increased from 30 to 60 mL/min, the dTMP/dT was quite similar. This result suggested that further increasing air flow rate above 30 mL/min was not able to reduce membrane fouling significantly in the hybrid process of coagulation-UF with air sparging, and similar results have been reported in bubbling-membrane filtration hybrid processes by other researchers (Xia *et al.* 2013). In Figure 3(a), the depicted TMP lines at the air flow rates of 0 and 15 mL/min intersected because the air sparging changed the fouling mechanisms. Due to the floc breakage caused by the direct strike and tangential shear stress induced by bubbles, the floc size decreased while the fractal dimension increased, leading to the formation of a tighter cake layer (Barbot *et al.* 2008; Liu *et al.* 2014). In contrast, no floc breakage happened in the case of no aeration, indicating the cake layer was loose. Moreover, the low air flow rate of 15 mL/min had limited influence on reducing membrane fouling. Therefore, within the first 6 hours, the growth of TMP was greater at the air flow rate of 15 mL/min than that at the air flow rate of 0. However, the air sparging led to a continuous erosion of surface fouling, while the cake layer was being compacted without aeration. Thus, the growth of TMP gradually slowed down at the air flow rate of 15 mL/min but remained fast under no aeration, causing the intersection of the two lines.

Figure 3(b) shows the TMP buildups varied at different aeration conditions under intermittent mode. Under the mode of 40-min aeration per hour, the dTMP/dT were decreased from 0.54 and 0.47 kPa/h by increasing the air flow rate from 30 to 60 mL/min. Similarly, under the mode of 30-min aeration per hour, the dTMP/dT at the air flow rate of 30 and 60 mL/min were 0.73 and 0.50 kPa/h, respectively. As a result of the different dTMP/dT, the difference in TMP buildups might be quite significant in long-term operation although it was not obvious after an 8 h filtration. Additionally, the TMP buildups changed slightly as the air flow rate increased from 30 to 60 mL/min under two intermittent modes. This was expected as the size distributions of bubbles and water qualities at air flow rates of 30 and 60 mL/min were both similar. Differences in TMP buildups between air flow rates of 30 and 60 mL/min were more

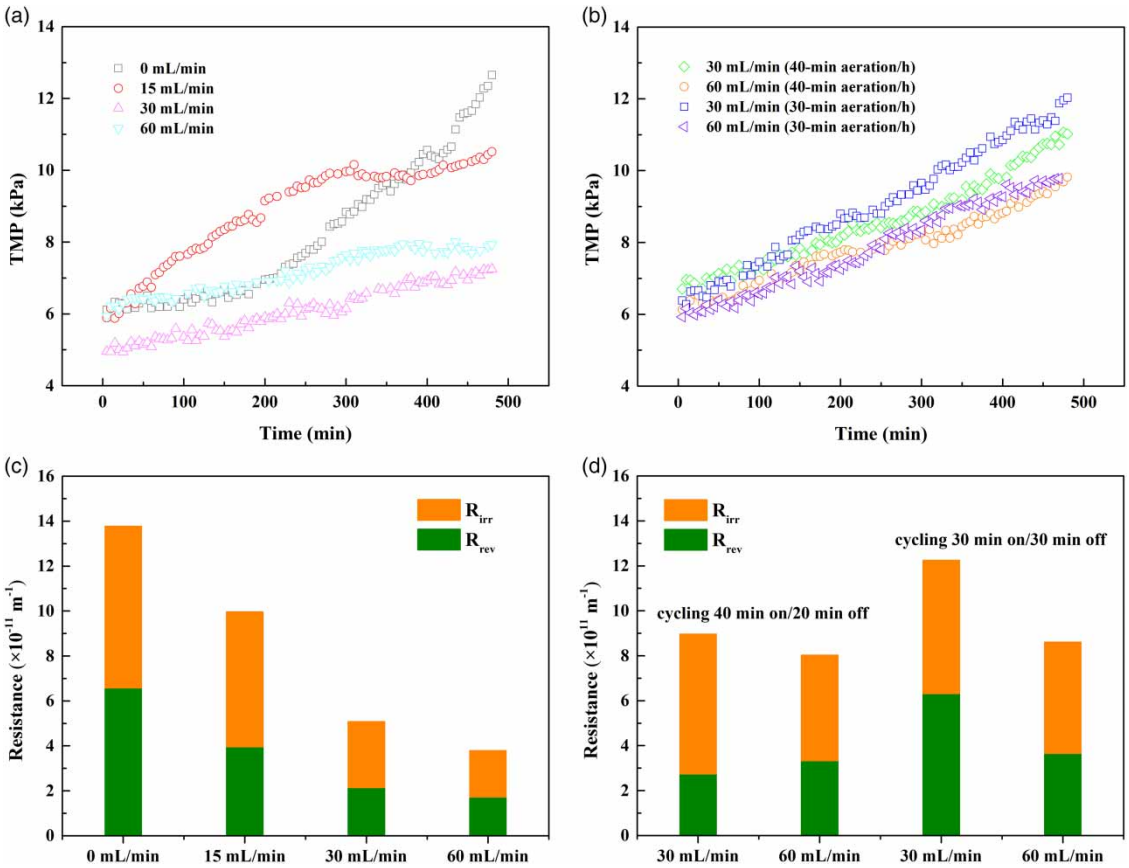

Figure 3 | Effect of air flow rate on TMP buildups (a) and (b) and membrane fouling resistances (c) and (d) under continuous sparging: (a) and (c) and intermittent sparging: (b) and (d).

obvious in the mode of 30-min aeration per hour than in the mode of 40-min aeration per hour. This discrepancy will be discussed below.

Figure 3(a) and 3(b) also illustrate the effect of aeration mode on TMP buildup. For a given air flow rate, TMP increased at a much slower rate with continuous sparging compared with intermittent one, which suggested that membrane fouling was better controlled under continuous sparging mode. There were two reasons for the more severe fouling under intermittent mode. First, water qualities were expected to be less advantageous with intermittent sparging than those with continuous one for a given air flow rate because flocs could not be transported out of the inner column during the pauses. Second, the effects of shear stresses on mitigating fouling were limited when aeration was periodically employed. In addition, the dTMP/dT increased as the aeration time per hour shortened from 40 to 30 min for a given air flow rate because the shorter sparging time resulted in more foulants accumulating on the membrane surface and decreasing the total number of shear stresses. Furthermore, when air flow rate increased from 30 to 60 mL/min, the dTMP/dT decreased by 31.5% in the mode of 30-min aeration per hour, whereas the dTMP/dT decreased by 13.0% in the mode of 40-min aeration per hour. These results suggested that the effect of air flow rate on TMP buildup was more remarkable in the mode of 30-min aeration per hour. In this mode, membrane fouling was more severe due to the less favorable shear stress conditions and water qualities. Hence, the reduction of fouling was more obviously observed as the air flow rate increased, according to the study of Sur & Cui (2001) that suggested membrane performance could be most significantly improved by aeration when the cake layer or the polarization fouling was more severe.

Figure 3(c) and 3(d) show the membrane fouling resistances under various aeration conditions. Under the

continuous sparging mode, the reversible resistance declined with the incremental air flow rate (Figure 3(c)). The reduction of reversible resistance was mainly due to the elimination of fouling layer on membrane surface by aeration. As also presented in Figure 3(c), the irreversible resistance was reduced by increasing air flow rate. There was a transition for the fouling layer from initially reversible to irreversible fouling during the long-term operations as reported by Peldszus *et al.* (2011). Thus, the alleviated irreversible resistances might be related to the retarded transitions of fouling type by continuous aeration. Under the intermittent sparging mode (Figure 3(d)), total fouling resistance at air flow rate of 30 mL/min (8.97×10^{11} m^{-1}) was slightly different from that at air flow rate of 60 mL/min (8.03×10^{11} m^{-1}) in the mode of 40-min aeration per hour. However, as air flow rate increased from 30 to 60 mL/min in the mode of 30-min aeration per hour, the decline of total fouling resistance from 12.25×10^{11} m^{-1} to 8.61×10^{11} m^{-1} was much more significant. These results can be explained by the summarization in the review made by Cui *et al.* (2003). The improvement in membrane performance was more significant when the total fouling resistance was increased.

Optimization of air sparging

Under the continuous sparging mode, the energy consumption of air sparging at the air flow rate of 15, 30, and 60 mL/min was 17.66, 35.22, and 70.63 J, respectively. The energy consumption at the air flow rate of 60 mL/min was two times the energy consumption at the air flow rate of 30 mL/min, while the fouling rates at these two air flow rates were almost the same. This result suggested that the air flow rate of 30 mL/min was more efficient in reducing membrane fouling. When air flow rate was 15 mL/min, although the dTMP/dT (0.58 kPa/h) was two times as much as that at 30 mL/min (0.29 kPa/h), the energy consumption was only half of that at 30 mL/min. Weighing the extents of fouling and energy consumption, the optimum air flow rates were from 15 to 30 mL/min under the continuous mode.

As for the intermittent aeration, the best membrane fouling control was achieved at the air flow rate of 60 mL/min in the mode of 40-min aeration per hour. However, the energy consumption (47.09 J) was high. In contrast, at the air flow rate of 30 mL/min in the mode of 40-min aeration per hour, the dTMP/dT (0.54 kPa/h) was similar to that at air flow rate of 15 mL/min in continuous mode (0.58 kPa/h) and the energy consumption (23.54 J) was within the acceptable range of 17.66–35.32 J. Hence, this condition can be another optimal choice. When the aeration was conducted under the mode of 30-min aeration per hour, the energy consumption at the air flow rates of 30 and 60 mL/min were the same as those at 15 and 30 mL/min in the continuous mode, respectively. Unfortunately, the dTMP/dT under the former two conditions were 0.73 and 0.50 kPa/h, which were much higher than the 0.58 and 0.29 kPa/h under the latter two conditions. As a result, air sparging in the mode of 30-min aeration per hour was not recommended.

CONCLUSIONS

To optimize the aeration conditions in the hybrid process of coagulation-UF with air sparging, we mainly investigated the effects of aeration conditions on membrane fouling. The conclusions can be drawn as follows:

1. The water quality including turbidity and UV_{254} of water that directly contact membranes were lowered in the presence of air sparging. More favorable shear stress profiles and better water qualities were responsible for the less severe fouling in the hybrid process.
2. Increasing air flow rates led to the generation of more bubbles with a wider size range, and membrane fouling could be effectively controlled regardless of aeration modes. Further increasing air flow rate was not able to achieve a significant reduction of fouling under continuous sparging mode.
3. The continuous sparging mode was more effective in eliminating membrane fouling than the intermittent one. For intermittent sparging, a longer aeration resulted in less membrane fouling. The mode of 40-min aeration per hour was superior to that of 30-min aeration per hour.
4. Weighing the energy consumption and the extents of membrane fouling, the optimum aeration conditions went to air flow rates between 15 and 30 mL/min with

continuous sparging and 30 mL/min in the mode of 40-min aeration per hour in this study.

ACKNOWLEDGEMENTS

This research was supported by the National Natural Science Foundation of China (Grant numbers: 51278317 and 51678377), Key Projects in the Science & Technology Program of Hainan Province (zdkj2016022), Applied Basic Research of Sichuan Province (2017JY0238) and the Litree Purifying Technology Co., Ltd.

REFERENCES

Abdullah, S. Z., Wray, H. E., Bérubé, P. R. & Andrews, R. C. 2015 Distribution of surface shear stress for a densely packed submerged hollow fiber membrane system. *Desalination* **357**, 117–120.

Barbot, E., Moustier, S., Bottero, J. & Moulin, P. 2008 Coagulation and ultrafiltration: Understanding of the key parameters of the hybrid process. *Journal of Membrane Science* **325** (2), 520–527.

Chan, C. C. V., Bérubé, P. R. & Hall, E. R. 2007 Shear profiles inside gas sparged submerged hollow fiber membrane modules. *Journal of Membrane Science* **297**, 104–120.

Chan, C. C. V., Bérubé, P. R. & Hall, E. R. 2011 Relationship between types of surface shear stress profiles and membrane fouling. *Water Research* **45** (19), 6403–6416.

Chen, Y., Dong, B. Z., Gao, N. Y. & Fan, J. C. 2007 Effect of coagulation pretreatment on fouling of an ultrafiltration membrane. *Desalination* **204** (1–3), 181–188.

Choi, K. Y. & Dempsey, B. A. 2004 In-line coagulation with low-pressure membrane filtration. *Water Research* **38** (19), 4271–4281.

Cui, Z. F., Chang, S. & Fane, A. G. 2003 The use of gas bubbling to enhance membrane processes. *Journal of Membrane Science* **221**, 1–35.

Drews, A., Prieske, H., Meyer, E.-L., Senger, G. & Kraume, M. 2010 Advantageous and detrimental effects of air sparging in membrane filtration: bubble movement, exerted shear and particle classification. *Desalination* **250** (3), 1083–1086.

Guigui, C., Rouch, J. C., Durand-Bourlier, L., Bonnelye, V. & Aptel, P. 2002 Impact of coagulation conditions on the in-line coagulation/UF process for drinking water production. *Desalination* **147** (1–3), 95–100.

Howe, K. J. & Clark, M. M. 2006 Effect of coagulation pretreatment on membrane filtration performance. *Journal of American Water Works Association* **98** (4), 133–146.

Howe, K. J., Marwah, A., Chiu, K.-P. & Adham, S. S. 2006 Effect of coagulation on the size of MF and UF membrane foulants. *Environmental Science & Technology* **40**, 7908–7913.

Jermann, D., Pronk, W., Kägi, R., Halbeisen, M. & Boller, M. 2008 Influence of interactions between NOM and particles on UF fouling mechanisms. *Water Research* **42** (14), 3870–3878.

Kimura, K., Hane, Y., Watanabe, Y., Amy, G. & Ohkuma, N. 2004 Irreversible membrane fouling during ultrafiltration of surface water. *Water Research* **38** (14–15), 3431–3441.

Liu, J., Liu, B., Liu, T., Bai, Y. & Yu, S. 2014 Coagulation-bubbling-ultrafiltration: effect of floc properties on the performance of a hybrid process. *Desalination* **333**, 126–133.

Meng, X., Tang, W., Wang, L., Wang, X., Huang, D., Chen, H. & Zhang, N. 2015 Mechanism analysis of membrane fouling behavior by humic acid using atomic force microscopy: effect of solution pH and hydrophilicity of PVDF ultrafiltration membrane interface. *Journal of Membrane Science* **487**, 180–188.

Müller, S. & Uhl, W. 2009 Influence of hybrid coagulation-ultrafiltration pretreatment on trace organics adsorption in drinking water treatment. *Journal of Water Supply: Research and Technology – Aqua* **58** (3), 170–180.

Peldszus, S., Hallé, C., Peiris, R. H., Hamouda, M., Jin, X., Legge, R. L., Budman, H., Moresoli, C. & Huck, P. M. 2011 Reversible and irreversible low-pressure membrane foulants in drinking water treatment: identification by principal component analysis of fluorescence EEM and mitigation by biofiltration pretreatment. *Water Research* **45** (16), 5161–5170.

Rojas-Serrano, F., Perez, J. I. & Gomez, M. A. 2015 Integrated in-line coagulation-aerated ultrafiltration for drinking-water production: a case study from laboratory to pilot plant. *Journal of Environmental Science and Health Part A – Toxic/Hazardous Substances & Environmental Engineering* **50** (13), 1376–1385.

Sur, H. W. & Cui, Z. 2001 Experimental study on the enhancement of yeast microfiltration with gas sparging. *Journal of Chemical Technology and Biotechnology* **76** (5), 477–484.

Tian, J.-y., Xu, Y.-p., Chen, Z.-l., Nan, J. & Li, G.-b. 2010 Air bubbling for alleviating membrane fouling of immersed hollow-fiber membrane for ultrafiltration of river water. *Desalination* **260** (1–3), 225–230.

Xia, L., Law, A. W.-K. & Fane, A. G. 2013 Hydrodynamic effects of air sparging on hollow fiber membranes in a bubble column reactor. *Water Research* **47** (11), 3762–3772.

Yamamura, H., Kimura, K. & Watanabe, Y. 2007 Mechanism involved in the evolution of physically irreversible fouling in microfiltration and ultrafiltration membranes used for drinking water treatment. *Environmental Science & Technology* **41** (9), 6789–6794.

Yeo, A. P. S., Law, A. W. K. & Fane, A. G. 2006 Factors affecting the performance of a submerged hollow fiber bundle. *Journal of Membrane Science* **280**, 969–982.

First received 27 April 2017; accepted in revised form 12 September 2017. Available online 19 October 2017